

PAPER • OPEN ACCESS

Ablation morphology and redistribution layer of gold films with different substrates irradiated by femtosecond laser pulse

To cite this article: Zhijie Xu 2019 *IOP Conf. Ser.: Mater. Sci. Eng.* **569** 022027

View the [article online](#) for updates and enhancements.

Ablation morphology and redistribution layer of gold films with different substrates irradiated by femtosecond laser pulse

Zhijie Xu^{1*}

¹ Laser Micro/Nano Fabrication Laboratory, School of Mechanical Engineering, Beijing Institute of Technology, Beijing, 100081, P. R. China

*Corresponding author's e-mail: 2120160439@bit.edu.cn

Abstract. Gold micro/nanostructure is of great significance in many scientific and engineering fields for its unique optical, electrical and thermal properties. Gold film deposited through electron beam (EB) evaporation is a suitable raw material for the fabrication of gold micro/nanostructure. Femtosecond laser directing is one of the reported methods for high-efficiency and low-cost micro/nanofabrication. We present a comparative study of gold film ablation with different substrates (Si, SiO₂, ZnO) under the irradiation of single femtosecond Gaussian pulse. The morphologies of ablation areas and redistribution layers are investigated by many characterization methods, such as scanning electron microscopy (SEM) and atomic force microscopy (AFM). In general, the ablation morphology and the ablation hole are mainly affected by the bandgap. Besides, the heat conductivity is the main factor affecting the width and height of the redistribution layer.

1. Introduction

Over last decades, gold micro/nanostructure is widely applied to many research fields, such as nanophotonics[1], biosensing[2] and optics[3] due to its ability to manipulate and confine incident light through localized surface plasmon resonance (LSPR). Pre-deposited gold film with dozens of nanometers through EB evaporation is an ideal tool for subsequent fabrication because of its low roughness and high uniformity[4]. Conventionally, the electron beam lithography (EBL)[5] and focused ion beam (FIB)[6] methods are the commonest methods adopted for nanostructure patterning based on gold film. However, these methods often suffer from the requirement of vacuum and complex fabrication steps like resist coating, photolithography, lift-off, and wet processing. All the mentioned drawbacks may lead to the low efficiency and repeatability[7].

Instead, femtosecond laser directing is considered as a vacuum-free and one-step micro/nano fabrication[8] method. Commonly, the redistribution layer is considered as a defect of laser processing because of the heating effect. However, due to the small heating effect during femtosecond laser patterning material, the tiny redistribution provides an alternative way for micro/nano fabrication. There exist many reported researches on gold film fabrication using femtosecond laser inducing redistribution layer. A. Wang, et al. reported a method for high-conductivity gold nanowire fabrication on gold film by spatially modulated femtosecond laser pulses[9]. W. Han, et al. reported a method for gold nanoparticles fabrication on gold film induced by dual wavelength femtosecond laser[10]. Generally, the gold film patterning using femtosecond laser irradiation is mostly based on the laser inducing material redistribution[11]. Wherein, the properties of substrate materials greatly affect the



material redistribution during the laser interaction. However, to my knowledge, the researches focusing on substrate materials are still scarce.

In this study, we demonstrate a comparative study of the morphologies of ablation areas and the sizes of redistribution layers with different gold film substrates. Considering the variation of bandgap and heat conductivity, three kinds of commonest substrates: Si, SiO₂, ZnO were taken into investigation. The structure parameters were measured using SEM and AFM. The cross sections of the ablation areas were collected and compared. The bandgap and threshold were found to significantly affect the ablation morphologies and ablation holes. Besides, the width and height of the redistribution layer relied on the capacity of heat-transmission.

2. Experimental setup

The experimental setup is shown in figure 1. The fundamental Gaussian mode with a central wavelength of 800 nm, and a pulse duration of 50 fs is generated by a regenerative amplifier system (Spitfire Ace-35F, Spectra Physics) whose gain medium is Ti:sapphire. The repetition rate could be adjusted from 1 Hz to 1000 Hz flexibly. The beam diameter($1/e^2$) of the laser is set as 7 mm before entering the objective lens. A half-wave plate and a polarizer are used to form an energy control system, and an objective lens (20×, NA = 0.45) is applied to achieve higher fluence and smaller spot size at the focusing plane. The sample is mounted on a computer-controlled, six-axis translation stage (M-840.5DG, PI, Inc.) with a resolution of 1 μm in x/y plane and 0.5 μm in z direction. The stage is omitted in the figure.

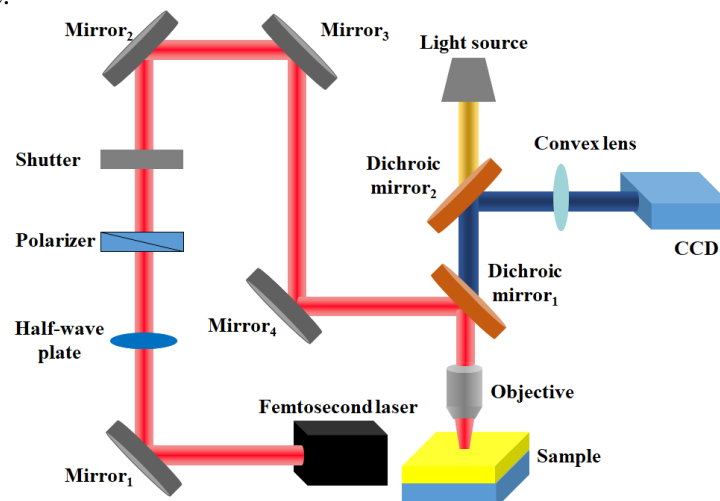


Figure 1. Experimental setup.

Thickness of the samples used in this study was 30 nm (with 3 nm Ti linking layer). To investigate the morphology changes of gold film, single pulse was applied to process the target gold film. The pulse energies were adjusted from 0.2 μJ to 1.2 μJ to achieve different structure parameters. The morphologies of the ablation areas were characterized using a field-emission scanning microscope (JSM-7500F, JEOL, Japan) and the cross section structure parameters were illustrated by the atomic force microscopy (Dimension Edge PSS, Bruker, Inc.).

3. Results and discussion

The ablation results fabricated by single Gaussian pulse with energy of 1.0 μJ are shown in figure 2. The sizes of ablation areas with different substrates are close to each other. This phenomenon is mainly attributed to Gaussian distribution of femtosecond laser and threshold effect in processing. According to the previous research, the diameter of the ablation area D can be expressed as[12]: $D^2 = 2\omega^2 \ln(F / F_{th})$, where ω is the waist radius of the Gaussian beam, F the peak density and F_{th} the ablation threshold of the material. Thus, the diameter of ablation area is not significantly affected by the peak density, and is mainly restricted by ablation threshold.

Besides, the redistribution layers of ablation areas are compared. The redistribution layer of the Si substrate is the most irregular. The SiO₂ substrate shows better material redistribution than Si substrate. The redistribution layer of ZnO substrate is orderly so that it is not obvious using the SEM from the vertical angle. In addition, due to the influence of the linear polarization, the distribution of redistribution layer is not uniform. As the femtosecond laser used in this study is linearly polarized, the ablation area is apparently elliptical rather circular. Specially, as far as the SiO₂ substrate, there are some periodical spatters around the redistribution layer due to the onset of some hydrodynamic instability[13]. The redistribution layer collapses at some margins of the ablation area.

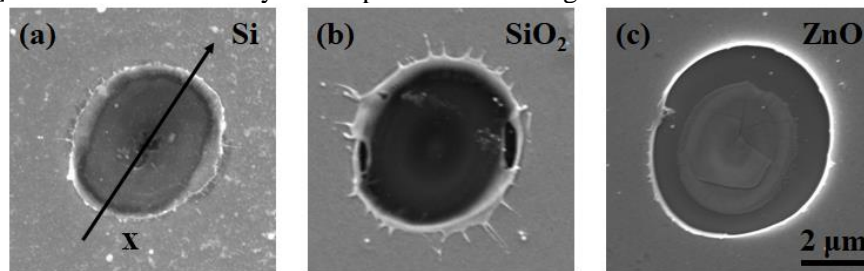


Figure 2. SEM images of gold film ablation with different substrates. The pulse energy is 1 μJ . (a) Si; (b) SiO₂; (c) ZnO.

In order to further investigate the morphologies of the ablation areas, the AFM image is used to measure the structure parameters. The AFM images of different substrates under several pulse energies are shown in figure 3. For all kinds of substrates, the size of the ablation area increases with the improving of pulse energy. When the pulse energy is fixed, the ablation size of Si substrate is smaller than that of SiO₂ substrate, which is smaller than that of ZnO substrate. Due to the Gaussian distribution, there is an ablation hole in the centre of the irradiation area. And when the substrate is Si, the depth of ablation hole is much deeper than that of the others. But the depths of ablation holes are close to each other when the substrates are SiO₂ and ZnO. This phenomenon would be discussed later.

Besides, the heights of the redistribution layer vary greatly when using different substrates. The layer height of SiO₂ substrate is obviously lower than the Si and ZnO. However, although the heights of redistribution layers are close when the substrates are Si and ZnO, the uniformity changes significantly. The polarization also affects the material redistribution. Taking the Si substrate as an example, more material redistribution is on both sides of the direction of the polarization. Specially, when the pulse energy is around 0.5 μJ , and the substrate is ZnO, there is a helical structure formation which may be attributed to the high-order harmonic generation during the laser irradiation[13,14].

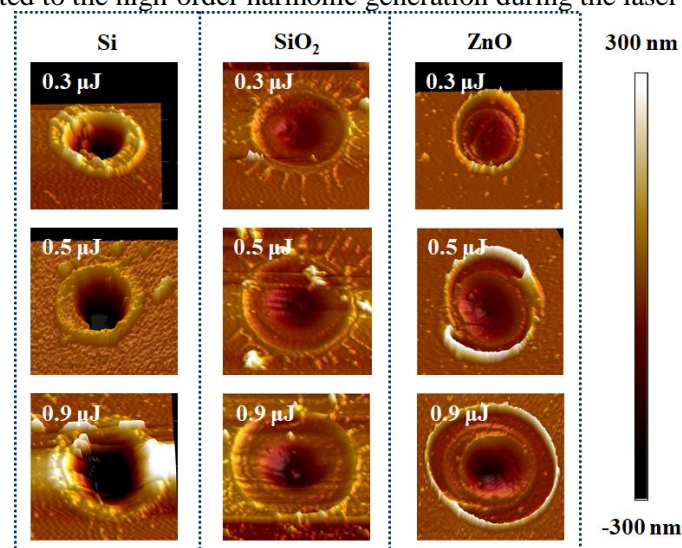


Figure 3. AFM images of gold film with different substrates. The pulse energies are marked in the figures.

To better measure the structure parameters changes of the femtosecond laser inducing morphologies, the cross sections data were collected. As illustrated in figure 4a, the curves confirm the result mentioned above that the ablation hole of Si substrate is much deeper than the others, which could reach 600 nm under the pulse energy of 0.3 μJ . The data of redistribution layer widths which are collected by changing the pulse energy from 0.2 μJ to 1.2 μJ are shown in figure 4b. The widths of Si and ZnO substrate redistribution layers are both much larger than SiO_2 substrate.

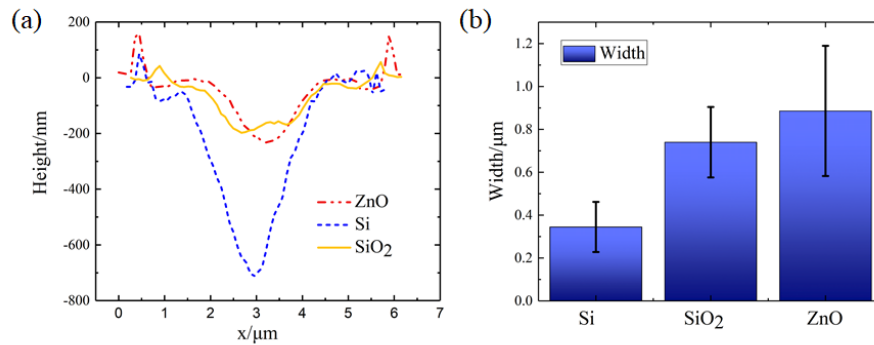


Figure 4. (a) Cross sections of the ablation areas using different substrates and the pulse energy is 0.3 μJ . (b) The widths of redistribution layers using different substrates with the energy from 0.2 μJ to 1.2 μJ .

To understand the mechanism of the difference formation when femtosecond laser irradiates the different substrates, the energy deposition during the interaction between femtosecond laser and gold film is discussed. The depth l_s that the femtosecond laser can reach is written as follow: $l_s = \frac{1}{\alpha}$, where α is the absorption coefficient which is related to the wavelength. The absorption coefficient of gold is $7.7089 \times 10^5 / \text{cm}$ when irradiated by 800 nm laser. Thus the depth $l_s = 1.2972 \times 10^3 \text{ nm}$. Then during the laser irradiation, the laser energy can gradually enter the depth of thermal diffusion l_d , which can be written as: $l_d = \sqrt{D\tau}$, where D is the thermal diffusivity and τ is the pulse duration. The thermal diffusivity D can be written as: $D = \frac{\lambda}{\rho c}$, where λ is the thermal conductivity, ρ the density and c the specific heat capacity. The thermal conductivity λ of gold is 318 W/(m·K), density ρ is 19.30 g/cm³ and specific heat capacity c is 0.13 kJ/(kg·K). Thus the thermal diffusivity D of gold is $1.267 \times 10^{-4} \text{ m}^2/\text{s}$ and the depth of thermal diffusion l_d is 0.3184 nm. So the depth of thermal diffusion $l_d \ll$ deposition depth l_s . The heat was deposited before it had time to diffuse during the interaction between femtosecond laser and gold film, which finally induced smaller redistribution layer[15].

Besides, the relevant physical characteristics of the used substrates, having fundamental impact on the morphologies, are listed below:

Table 1. Relevant physical characteristics of the used substrates.

	Bandgap/eV	Thermal conductivity/ W/(m·k)
Si	1.12	149
SiO ₂	9	12/6.8/1.4
ZnO	3.3	30

As can be calculated, the energy of femtosecond laser photon used in this study is 1.55 eV, which is higher than Si but lower than SiO₂ and ZnO. Thus, the interactions between laser and SiO₂ and ZnO substrate both involve in complex nonlinear effect, which leads to the difficulty in processing deep hole and similar ablation hole depth. Besides, the thermal conductance of SiO₂ is much weaker than the others. The better thermal conductance could induce more material melting and accumulation, which finally leads to the wider and higher redistribution layer.

4. Conclusion

In summary, gold films with different kinds of substrates (Si, SiO₂ and ZnO) are irradiated by the femtosecond Gaussian pulses. The ablation area morphologies and redistribution layers are measured using SEM and AFM. Besides the polarization of the laser, the physical characteristics like bandgap and thermal conductivity are considered to notably affect the ablation results. The ablation hole is the deepest and the morphology is most irregular when Si substrate is processed because of its narrowest bandgap. The redistribution layer of SiO₂ substrate is relatively small for its relatively poor thermal conductance. This research fundamentally supports the laser patterning gold film micro/nanostructure, paving the way for its wide applications in optical and optoelectronic devices.

References

- [1] A. Kuchmizhak, S. Gurbatov, O. Vitrik, Y. Kulchin, V. Milichko, S. Makarov and S. Kudryashov, (2016), Ion-Beam Assisted Laser Fabrication of Sensing Plasmonic Nanostructures, *Sci Rep-Uk* **6**.
- [2] D. K. Lim, K. S. Jeon, H. M. Kim, J. M. Nam and Y. D. Suh, (2010), Nanogap-Engineerable Raman-Active Nanodumbbells for Single-Molecule Detection, *Nat Mater* **9** (1), 60-67.
- [3] S. Kim, J. H. Jin, Y. J. Kim, I. Y. Park, Y. Kim and S. W. Kim, (2008) High-Harmonic Generation by Resonant Plasmon Field Enhancement, *Nature* **453** (7196), 757-760.
- [4] G. F. S. Andrade, J. G. Hayashi, M. M. Rahman, W. J. Salcedo, C. M. B. Cordeiro and A. G. Brolo, (2013) Surface-Enhanced Resonance Raman Scattering (Serrs) Using Au Nanohole Arrays on Optical Fiber Tips, *Plasmonics* **8** (2), 1113-1121.
- [5] J. Zhang, M. Irannejad and B. Cui, (2015) Bowtie Nanoantenna with Single-Digit Nanometer Gap for Surface-Enhanced Raman Scattering (Sers), *Plasmonics* **10** (4), 831-837.
- [6] M. Horak, K. Bukvisova, V. Svarc, J. Jaskowiec, V. Krapek and T. Sikola, (2018) Comparative Study of Plasmonic Antennas Fabricated by Electron Beam and Focused Ion Beam Lithography, *Sci Rep-Uk* **8**.
- [7] V. Dubois, F. Niklaus and G. Stemme, (2016) Crack-Defined Electronic Nanogaps, *Adv Mater* **28** (11), 2178-2182.
- [8] L. Jiang, A. D. Wang, B. Li, T. H. Cui and Y. F. Lu, (2018) Electrons Dynamics Control by Shaping Femtosecond Laser Pulses in Micro/Nanofabrication: Modeling, Method, Measurement and Application, *Light-Sci Appl* **7**.
- [9] A. D. Wang, L. Jiang, X. W. Li, Y. Liu, X. Z. Dong, L. T. Qu, X. M. Duan and Y. F. Lu, (2015) Mask-Free Patterning of High-Conductivity Metal Nanowires in Open Air by Spatially Modulated Femtosecond Laser Pulses, *Adv Mater* **27** (40), 6238-6243.
- [10] W. N. Han, L. Jiang, X. W. Li, Q. S. Wang, S. J. Wang, J. Hu and Y. F. Lu, (2017) Controllable Plasmonic Nanostructures Induced by Dual-Wavelength Femtosecond Laser Irradiation, *Sci Rep-Uk* **7**.
- [11] A. D. Wang, L. Jiang, X. W. Li, Z. J. Xu, L. L. Huang, K. H. Zhang, X. Ji and Y. F. Lu, (2017) Nanoscale Material Redistribution Induced by Spatially Modulated Femtosecond Laser Pulses for Flexible High-Efficiency Surface Patterning, *Opt Express* **25** (25), 31431-31442.
- [12] J. M. Liu, Simple Technique for Measurements of Pulsed Gaussian-Beam Spot Sizes, (1982) *Opt Lett* **7** (5), 196-198.
- [13] H. Cao, J. Y. Wu, H. C. Ong, J. Y. Dai and R. P. H. Chang, (1998) Second Harmonic Generation in Laser Ablated Zinc Oxide Thin Films, *Appl Phys Lett* **73** (5), 572-574.
- [14] G. I. Petrov, V. Shcheslavskiy, V. V. Yakovlev, I. Ozerov, E. Chelnokov and W. Marine, (2003) Efficient Third-Harmonic Generation in a Thin Nanocrystalline Film of ZnO, *Appl Phys Lett* **83** (19), 3993-3995.
- [15] M. D. Shirk and P. A. Molian, (1998) A Review of Ultrashort Pulsed Laser Ablation of Materials, *J Laser Appl* **10** (1), 18-28.